



# F44 Zeeman Spectroscopy

## Short Report

Nils Schmitt

Timo Kleinbek

Conducted in August 2018

Supervisor: Srinivas, Hemkumar

**Abstract** *The Zeeman effect is an atomic physics phenomenon that describes how spectral lines of an element are split when the magnetic moment of the atom is coupled to an external magnetic field. The aim of this experiment was to observe the normal Zeeman effect in cadmium and then to investigate the splitting of the spectral lines as a function of the magnetic field strength. In the second part of the experiment we determine the wavelength of the red cadmium line by using a Czerny-Turner spectrometer. We also had to determine the spectral line of an unknown element, which unfortunately was not possible because we could not resolve it. In our measurement we determined only the wavelength  $\lambda_{\text{Cd}} = (643.8 \pm 2.9) \text{ nm}$ . In addition, the Bohr magneton  $\mu_B$  could be calculated from both test parts, for which we obtained the value  $\mu_B = (9.7 \pm 0.8) \times 10^{-24} \text{ J/T}$ .*

## 1. Introduction

The Zeeman effect was studied first in 1896 by the Dutch physicist Peter Zeeman when he observed the widening of the yellow D-lines of burning sodium between strong magnets. Later he found out that the widening of the lines was actually a division in up to 15 components.

The spectral lines of an element arise when an electron emits a photon at the transition between different energy levels, whose wavelength depends on the energy difference between the levels. If a strong external magnetic field is applied, individual energy levels are changed by coupling the magnetic moment of the electron with the external magnetic field, which leads to a splitting of the spectral lines. A distinction is made between the normal Zeeman effect observed in the experiment and the anomalous Zeeman effect. These differ in the total spin  $S$  of the electron, which is  $S = 0$  at the normal Zeeman effect and  $S \neq 0$  at the anomalous Zeeman effect.

## 2. Theoretical Basics

### Normal Zeeman effect

To understand the basics of the Zeeman effect, we first assume that the magnetic moment of an electron  $I$  can be sufficiently described by Bohr's atomic model.

According to this model, the electron orbits the atomic nucleus as point mass  $m_e$  with velocity  $v$  and charge  $e$  at a distance  $r_B$ , the Bohr radius. Using this approximation, the orbital magnetic mo-

ment

$$\boldsymbol{\mu}_l = \frac{evr}{2} \cdot \mathbf{n} \quad (1)$$

is obtained.

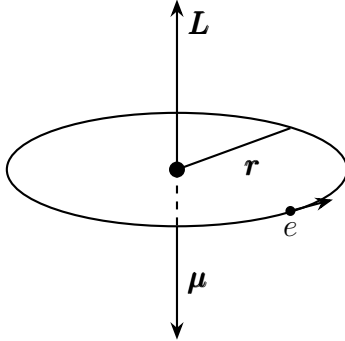


Figure 1: Bohr model of an electron with the angular momentum  $\mathbf{L}$  and the magnetic moment  $\boldsymbol{\mu}$

Thus  $\mathbf{n}$  is the normal vector, perpendicular to the disk on which the electron moves (see Fig. 1).

You can easily see that the magnetic moment resembles the angular momentum of the electron

$$\mathbf{l} = \mathbf{r} \times \mathbf{p} = m_e r v \cdot \mathbf{n}. \quad (2)$$

If an external magnetic field  $\mathbf{B}$  is applied, it interacts with the magnetic moment of the electron so that the energy level

$$\Delta E_{\text{pot}} = -\boldsymbol{\mu}_l \cdot \mathbf{B} = \frac{e}{2m_e} \cdot \mathbf{l} \cdot \mathbf{B} \quad (3)$$

changes.

Now the angular momentum of the electron along the magnetic field vector  $\mathbf{B}$  is quantized in the form

$$|\mathbf{l}| = \sqrt{l(l+1)}\hbar \quad (4)$$

with the quantum number  $l = 0, 1, \dots, n-1$  and the  $z$ -component

$$l_z = m_l \hbar, \quad (5)$$

which runs in the range  $-l \leq m_l \leq l$ .

This allows you to simplify the energy difference to

$$\Delta E_{\text{pot}} = \frac{e\hbar}{2m_e} m_l B = \mu_B m_l B, \quad (6)$$

where  $\mu_B$  describes the Bohr magneton we are looking for.

(1) Changing the energy level by  $\Delta E_{\text{pot}}$  causes the original energy level with angular momentum  $l$  to split into  $2l+1$  lower levels with the same angular momentum  $l$  but different  $m_l$  (see Fig. 2).

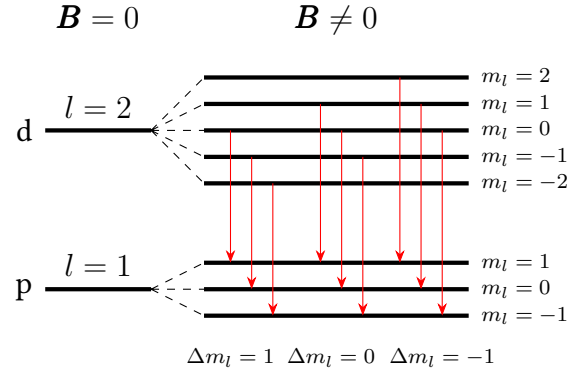


Figure 2: Schematic of the energy levels through the normal Zeeman effect

Alternatively, this equation can also be derived quantum mechanically. All spins and torques of the electrons in an atom are considered as individual sums, as well as the total spin  $\mathbf{J}$  required for the Hamilton operator in the external magnetic field.

This gives the equation

$$\Delta E_{\text{pot}} = \mu_B \cdot M_J \cdot B \cdot g_j \quad (7)$$

with the Landé factor  $g_j$ , which is one for the normal Zeeman effect we needed. The matrix element  $M_J$  that appears in the equation is explained again in the following section.

### Selection Rules and polarization of light

When an electron “jumps” between two electron shells  $E_i$  and  $E_k$ , it emits a photon with a wavelength  $\lambda$ , which depends on the energy difference of the electron shells

$$\frac{hc}{\lambda} = E_{\text{photon}} = \Delta E = E_i - E_k. \quad (8)$$

However, there are restrictions on which transitions are possible. Important for this is the dipole

matrix element

$$M_{ik} = e \int \psi_i^* \mathbf{r} \psi_k dV, \quad (9)$$

which describes the transition probability between the electron shells  $k$  to  $i$ . It must also have at least one component other than zero for a transition from  $k$  to  $i$  to be possible.

If we evaluate the integral in three spatial directions, we get the conditions

$$\Delta M_J = M_{J,i} - M_{J,k} = 0, \pm 1, \quad (10)$$

$$\Delta L = L_i - L_k = \pm 1, \quad (11)$$

$$\Delta S = 0. \quad (12)$$

Assuming the magnetic field vector  $\mathbf{B}$  points in the  $z$ -direction, only the matrix element  $(M_{ik})_z$  cannot become zero for  $\Delta M_J = 0$ . These transitions are called  $\pi$  transitions. These are equivalent to a dipole oscillating along the  $z$ -axis, which means that no radiation is emitted along the  $z$ -direction. In the other two directions, this oscillation of the dipole can be observed as linearly polarized light.

If  $\Delta M_J = \pm 1$ , we get  $\sigma$  transitions, for which the  $z$ -component of the dipole matrix becomes zero and the  $x$ - and  $y$ -components are not equal to zero, but phase shifted to each other by  $\pi/2$ . This causes us to observe circularly polarized light along the  $z$ -axis and linearly polarized light along the  $x$ - and  $y$ -axis.

The direction of observation along the  $z$ -axis is called longitudinal and for  $\Delta M_J = +1$  and  $\Delta M_J = -1$  circular polarized  $\sigma$ -lines should be visible.

In contrast, linearly polarized  $\pi$ -lines should be observed in the transverse direction (perpendicular to the  $z$ -axis).

### 3. Measurements Log and Evaluation

#### First Part: Spectroscopy of the Zeeman effect

In the first part of the experiment, the Zeeman effect was investigated using the red cadmium line,

which is formed at the transition from  $^1D_2 \rightarrow ^1P_1$ .

To this end, it should first be examined whether a hysteresis effect occurs with the magnets used. For this purpose, three measurements were performed with a Hall probe each with increasing and decreasing field strength in the relevant range and the results for  $B_{\text{inc}}$  and  $B_{\text{dec}}$  were averaged. In Figure 3 you see the results of this measurement. You can see that there is a small difference

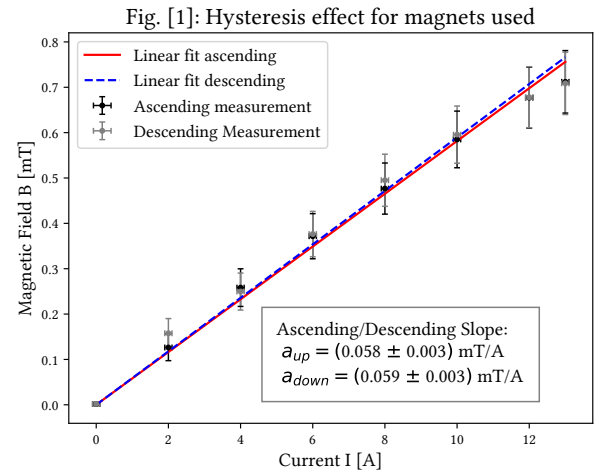


Figure 3: Comparison of the magnetic field strength with increasing and decreasing current strength

between the measurements, but the fit reveals that this difference is within the error, which is why in our case there is no significant effect.

Next, the Zeeman effect should be qualitatively investigated in longitudinal and transverse direction. For this purpose, we used the structure shown in figure 4. The most important element of this construction is the Lummer-Gehrcke plate with almost plane-parallel surfaces. If light enters the plate through a prism with an angle of incidence of  $\beta$ , it is reflected inside the plate. After each reflection some light is refracted at the surface, which is focused with the help of a lens and brought to interference.

If the path difference meets the conditions

$$\Delta_i = 2d\sqrt{n_i^2 - 1} = k\lambda \quad (13)$$

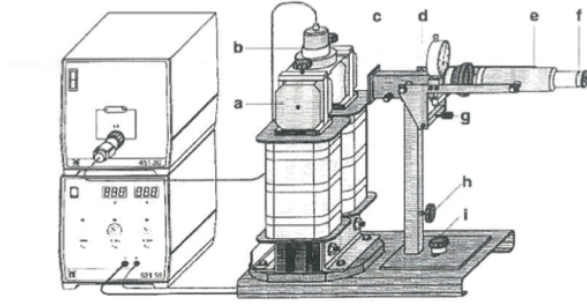


Figure 4: Experimental set-up: a) Pole pieces of the magnet, b) Cd lamp, c) Red light filter, d) Lummer-Gehrcke Plate, e) Telescope, f) Eyepiece, g) Height adjustment for the telescope, h) Locking screw for the telescope holder, i) Locking screw for the base plate. [2]

constructive interference with the path difference  $\Delta = \Delta_1 - \Delta_2$  is obtained. Therefore the refractive index is  $n = n_2$  and  $n_1 \approx 1$ , the thickness of the plate is  $d$  and the interference order is  $k$ . The reflection angle  $\alpha$  within the plate is assumed to be approximately  $90^\circ$ , resulting in near total reflection within the plate.

Our interference pattern of the Lummer-Gehrcke plate for a transversal image can be seen in Figure 5. The quantitative results from the obser-

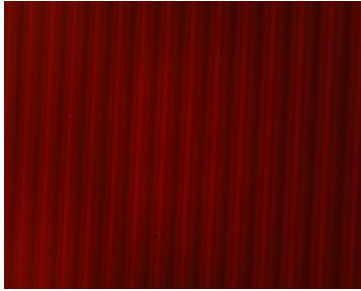
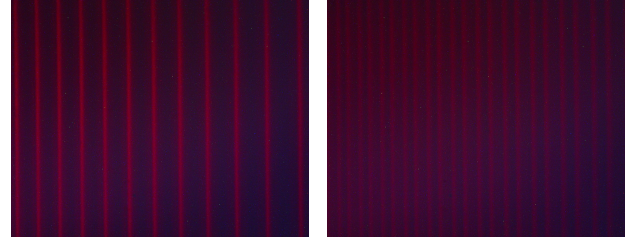


Figure 5: Zeeman effect with 13 A

vation of the Zeeman effect should next be used to determine Bohr's magneton. For this purpose, the images (e.g. Fig. 6) from the first test section were plotted in Python and fitted with a Gaussian function. This gave us the positions and width of the interference lines in pixels for each measurement with  $I = 9$  A, 11 A, 13 A. The orders of the  $\pi$ -lines were plotted against the position in pixels and provided with a second-order polynomial fit.



(a)  $\pi$ -lines

(b)  $\sigma$ -lines

Figure 6: Interference with 11 A

With the help of this fit the orders of the  $\sigma$ -lines were determined.

In order to determine Bohr's magneton, we consider the distance between the  $\pi$ - and  $\sigma$ -lines, which can identify the wavelengths as  $\lambda$  and  $\lambda + \delta\lambda$ . For  $\delta\lambda$  from the measurement

$$\delta\lambda = \frac{\delta k}{\Delta k} \cdot \Delta\lambda = \delta k \cdot \Delta\lambda \quad (14)$$

with  $\Delta k$  the order difference between two  $\pi$ -lines,  $\delta k$  the order difference between  $\pi$ - and  $\sigma$ -lines and  $\Delta\lambda$  determined by

$$\Delta\lambda = \frac{\lambda^2}{2d\sqrt{n^2 - 1}}. \quad (15)$$

Thus for  $\delta\lambda$  depending on  $\delta k$  the equation

$$\delta\lambda = \delta k \cdot \frac{\lambda^2}{2d\sqrt{n^2 - 1}} \quad (16)$$

results with  $n = 1.457$  and  $d = 4.04$  mm. For this measurement  $\lambda$  is the wavelength of the red cadmium line, which we determined as  $\lambda_{\text{Cd}} = (643.8 \pm 2.9)$  nm in the second part of the experiment. Using the energy difference  $E_{\text{pot}}$  of two wavelengths

$$\Delta E_{\text{pot}} = hc \left( \frac{1}{\lambda_1} - \frac{1}{\lambda_2} \right) \approx hc \cdot \frac{\delta\lambda}{\Delta\lambda} \quad (17)$$

and equates it with the energy difference of the associated energy levels (see Eq. 6), then one obtains

$$\mu_B = \frac{hc}{2Bd\sqrt{n^2 - 1}} \cdot \delta k. \quad (18)$$

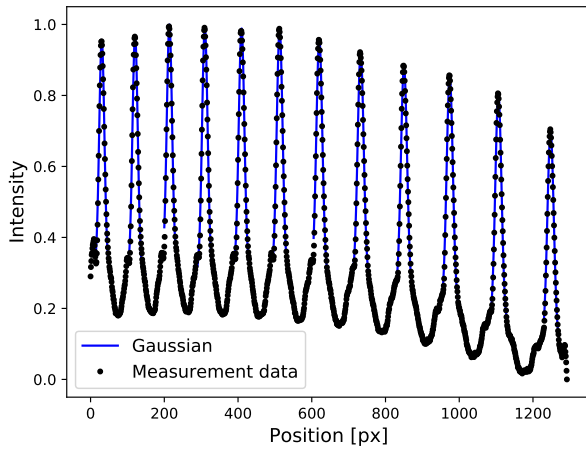
$I$ [A]	$B$ [T]	$\mu_B$ [ $10^{-24}$ J/T]
9	$0.527 \pm 0.019$	$10.1 \pm 1.5$
11	$0.644 \pm 0.023$	$9.8 \pm 1.5$
13	$0.761 \pm 0.027$	$9.7 \pm 0.8$

Table 1: Bohr's magneton for each current

In our experiment, a Bohr's magneton of

$$\mu_B = (9.7 \pm 0.8) \times 10^{-24} \text{ J/T}$$

is obtained, while the literature value is  $\mu_B = 9.274 \times 10^{-24} \text{ J/T}$  and the two values overlap in the  $1\sigma$ -range. The error results from error propagation on the standard deviation analogous to the standard deviation of the Gaussian peaks in Fig. 7 builds up.

Figure 7:  $\pi$ -lines with 11 A

### Second Part: Precision spectroscopy

In the second part of the experiment, the wavelengths of two lines of the cadmium spectrum were to be determined.

A Czerny-Turner spectrometer with a neon lamp as a reference was used for this purpose. The spectrometer allows the spectral acquisition of the wavelengths of incoming light with the aid of a grating. The light entering through an opening is focused through a concave mirror onto the

grating, where it is spectrally split and then reflected by another mirror so that the CMOS camera is in the focal plane of the spectrum.

First, we determined the position of the peaks in the neon spectrum in the range around 640 nm in a reference measurement. The peaks in the spectrum image were fitted with Gaussian functions in order to obtain the pixel positions for various wavelengths (see Fig. 8 and 9). The standard de-

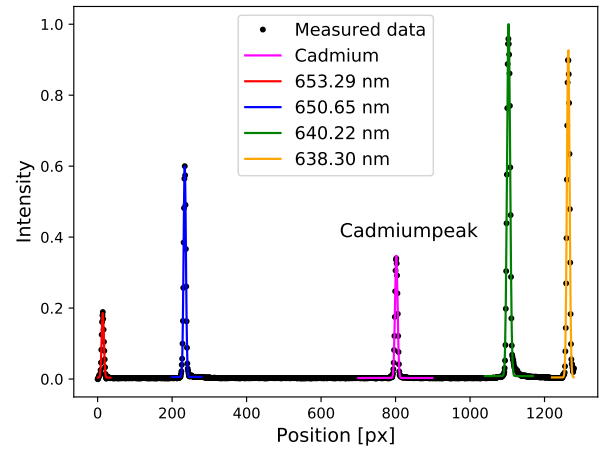


Figure 8: Spectrum of Cadmium and Neon

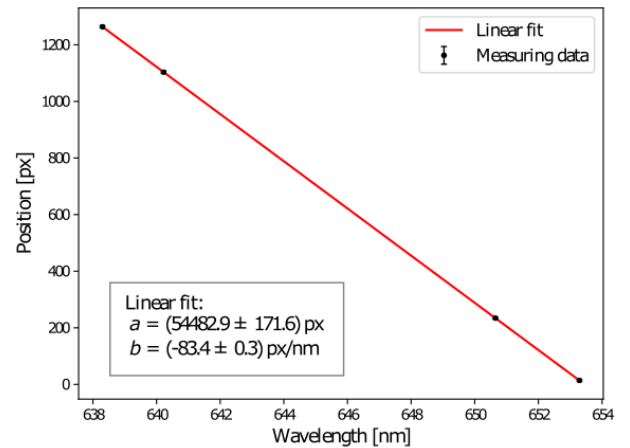


Figure 9: Position as function of the wavelength  
violation of the Gaussian Distribution was used as error.

In a second measurement, we recorded the spectrum of the cadmium lamp with the same settings



and also determined the position of the peaks using a Gaussian fit. From the fit of the first measurement we could then calculate the wavelengths of the two visible lines. For the strong cadmium line we obtained a wavelength of

$$\lambda_{\text{Cd}} = (643.8 \pm 2.9) \text{ nm.}$$

Unfortunately, we were no longer resolve another weak line. Nevertheless, it can be assumed that Xenon is to be seen as gaseous impurity or Tungsten as electrode material.

## 4. Critical Comment

The aim of the experiment was to determine the Bohr magneton using the Zeeman effect and then to determine the wavelengths of the red cadmium line and an unknown element using a Czerny-Turner spectrometer.

In the first part of the experiment, the magnet used was examined for hysteresis effects which, however, turned out to be negligible. The external errors, such as the manual insertion of the Hall probe, probably outweighed the corresponding measurements. Next, the Zeeman effect itself was observed qualitatively with a cadmium lamp. The polarization and the number of interference lines in longitudinal and transverse direction were investigated. The observations were consistent with the previous theoretical considerations. From the transverse direction of observation we could additionally obtain information about the line position and thus calculate Bohr's magneton. We have obtained an experimental value of  $\mu_B = (9.7 \pm 0.8) \times 10^{-24} \text{ J/T}$  that is not significantly different from the literature value  $\mu_{\text{B, lit}} = 9.274 \times 10^{-24} \text{ J/T}$ . Remarkable here is the large error of over 8% for the average of 3 measurements. The error results mainly from the inaccuracy of the fit curves, since the standard deviation was used as the error of the position of the peaks.

In the second part of the experiment, the wavelengths of cadmium and another element were to be determined. For the strong red cadmium line a wavelength of  $\lambda_{\text{Cd}} = (643.8 \pm 2.9) \text{ nm}$  was

obtained, which did not differ significantly from the literature value  $\lambda_{\text{Cd, lit}} = 643.8 \text{ nm}$ . Unfortunately, we could not see a line in the spectrum for the unknown element.

Overall, the test was therefore satisfactory, as all measured values in the error range corresponded to the literature values. As a possible improvement, we would suggest an optical bench for mounting the optical elements, which would reduce the number of inadvertent misalignments. On the other hand, mechanical mounting would be advantageous for the Hall probe, as the hysteresis effect would obviously be very small and thus a source of error could be eliminated.

## References

- [1] Wolfgang Demtröder. *Experimentalphysik 3. Atome, Moleküle und Festkörper*. ger. 5. Aufl. 2016. Springer-Lehrbuch. Berlin, Heidelberg: Springer Spektrum, 2016, Online-Ressource (XXI, 588 S. 740 Abb. in Farbe, online resource). ISBN: 978-3-662-49094-5. DOI: [10.1007/978-3-662-49094-5](https://doi.org/10.1007/978-3-662-49094-5). URL: <http://dx.doi.org/10.1007/978-3-662-49094-5>.
- [2] LD Didactic GmbH. *Physics Leaflets*. en. URL: [https://www.ld-didactic.de/literatur/hb/p\\_index\\_e.html#](https://www.ld-didactic.de/literatur/hb/p_index_e.html#) (visited on 08/18/2018).
- [3] MPIK. "Zeeman effect. FP instructions". en. In: (Mar. 10, 2012). URL: <https://www.phys.uni-heidelberg.de/Einrichtungen/FP/anleitungen/F44.pdf>.